

Optical detection of ligand electron–nuclear double resonance and the saturation of electron paramagnetic resonance in the ground state of the Tm^{2+} ion in CaF_2

S. A. Kazanskii

S. I. Vavilov State Optical Institute

(Submitted 1 August 1980)

Zh. Eksp. Teor. Fiz. **80**, 1469–1479 (April 1981)

The electron paramagnetic resonance and electron nuclear double resonance spectra of the Tm^{2+} ion in the ground state in CaF_2 are studied at $T = 1.8$ °K by an optical detection method based on magnetic circular dichroism in the absorption bands. The role of the dipole–dipole reservoir is clarified under conditions of saturation of the inhomogeneous EPR line of Tm^{2+} ion with restricted spectral diffusion. The relaxation parameters of the electronic spins in Tm^{2+} and the nuclear spins in the F^{19} surrounding the Tm^{2+} ions are estimated.

PACS numbers: 76.70.Dx, 76.30.Kg

1. INTRODUCTION

Development of methods for optical detection of electron paramagnetic resonance (EPR) and electron–nuclear double resonance (ENDOR) is of interest, since in certain cases^{1,2} the sensitivity of optical detection methods may significantly surpass the sensitivity of traditional methods. For the study of the ground states of paramagnetic centers, one of the most powerful optical detection methods (besides with Faraday rotation) is a method based on a measurement of the magnetic circular dichroism (MCD)^{1,2} in the absorption bands of the paramagnetic centers of a crystal situated in a constant magnetic field H_0 . MCD is the difference between the absorption coefficients of right- and left-circularly polarized light (measured in the geometry $H_0 \parallel L$, where L is the observation direction); in the case under consideration, it is a consequence of the Boltzmann population of the spin sublevels (split in the field H_0) of the ground states of the centers at low temperature. As a rule, a change in this population leads to a change in the MCD signal. It is interesting to note that the intensity of the optical-detection EPR spectrum, which is the dependence of the MCD on H_0 when the test sample is simultaneously exposed to a resonant microwave field, at least does not decrease with an increase in the microwave field. This allows us to study the EPR of such centers with “forbidden” transitions, which can not be observed with traditional methods (see, for example, Ref. 3); the possibility arises for the study of weak spin–spin coupling between paramagnetic impurities at low concentration^{4,5} etc. Optical detection methods also allow us to record the EPR signal when the EPR is highly saturated (in a strong microwave field),⁵ something difficult to do by traditional methods, and is of interest in connection with the problem of dynamic nuclear polarization.⁶

In this work we have studied the EPR and ENDOR of the ground state of the Tm^{2+} ion by an optical detection method based on the magnetic circular dichroism in the absorption band of the Tm^{2+} ion in CaF_2 . The saturation of the optical detection EPR line of the Tm^{2+} ion was studied as a function of the microwave field and estimates were made for the relaxation parameters char-

acterizing the coupling between the electronic and nuclear subsystems. Knowledge of these parameters is necessary for a study of the dynamic nuclear polarization under conditions of inhomogeneous broadening of the EPR line^{7,8}, especially since the Tm^{2+} ion is of interest in connection with this problem.⁵ Furthermore, despite the fact that the Tm^{2+} ion in fluorite crystals is the classical object for application of optical detection methods,¹ the ligand ENDOR spectrum during optical detection for this and other rare-earth ions has to our knowledge not been observed so far.

2. OBJECT, INVESTIGATION TECHNIQUE, AND EXPERIMENTAL RESULTS

In the EPR spectra of cubic Tm^{2+} centers in CaF_2 (Ref. 9), including optical detection EPR (Refs. 4, 10), two lines are observed which correspond to reorientation of the spin $|S_x| = 1/2$ of the $Tm^{2+} : 4f^{13}$ electron shell in a magnetic field H_0 ($g = +3.454$) in hyperfine interaction (interaction constant $A_{FS} = -1101$ MHz) with the nuclear moment ($|I_x| = 1/2$) of ^{169}Tm (100% abundance). The inhomogeneous broadening of the EPR line of the Tm^{2+} ion is connected with the scatter of the values of local field acting on the paramagnetic ion, due to the random orientation of the nuclear moments of several coordination spheres of the anion environment of the paramagnetic ion.

The ligand ENDOR spectra of Tm^{2+} in CaF_2 have been studied in Ref. 11 (operating frequency of the EPR spectrometer $\nu_1 = 24$ GHz). In that work, the constants A_S and A_P for the hyperfine interaction between the electron spin of the paramagnetic ion and the nuclear spins of the ligands were determined for the first four coordination spheres of the anion environment.

In our work, we studied CaF_2 crystals containing $n \sim 10^{18} \text{ cm}^{-3} Tm^{2+}$ ions at $T = 1.8$ °K (the concentration was determined from the absorbance in the characteristic absorption bands¹²), see Table I. Samples of dimensions $\sim 4 \times 4 \times 4$ mm were set in a TE_{011} microwave cavity ($\lambda = 3$ cm) and placed within a superconducting solenoid which generated the constant homogeneous magnetic field H_0 . The cavity was pierced by four pins placed parallel to the axis and forming a two-

TABLE I. Data on the studied $\text{CaF}_2:\text{Tm}^{2+}$ crystals and also estimates of some spin relaxation parameters.

	Samples		
	№ 1	№ 2	№ 3
$n(\text{Tm}^{2+}), \text{cm}^{-3}$ (in the batch)	$4.9 \cdot 10^{19}$?	$2.5 \cdot 10^{19}$
Reduction method	Radiative	Additive?	Radiative
$n(\text{Tm}^{2+}), \text{cm}^{-3}$	$1.0 \cdot 10^{18}$	$2.4 \cdot 10^{18}$	$0.5 \cdot 10^{18}$
Other paramagnetic impurities n, cm^{-3}	not observed	$10^{17} - 10^{18}$	not observed
EPR line width, G	18	25	—
T_2^{-1}, c^{-1}	$2.8 \cdot 10^6$	$(2.6 - 3.8) \cdot 10^6$	—
τ_1, c	$(3 \pm 1) \cdot 10^{-3}$	$(1 \pm 0.1) \cdot 10^{-1}$	$3.6 \cdot 10^{-2}$
τ_2, c	$(1 - 4) \cdot 10^{-7}$	$(0.1 - 1) \cdot 10^{-7}$	—
τ_3, c	$(1 - 3) \cdot 10^{-4}$	$\sim 10^{-4}$	—
$\alpha\omega_{SS}, \text{c}^{-2}$	$3.9 \cdot 10^{17}$	$(4.5 - 7.5) \cdot 10^{17}$	—
$(\beta_{SS}/\beta_L)_{\text{max}} (s \rightarrow \infty)$	44	32 - 40	—

turn radiofrequency coil (of the type in Ref. 13), insulated from the cavity. When a current of frequency 5–13 MHz was excited in the coil by a high-power generator, a sufficiently homogeneous rf field H_2 could be created at the sample with an amplitude up to ~ 2 G. The microwave power dissipated in the cavity could be reduced from $P_{\text{max}} = 85$ mW by a calibrated attenuator. The value of the microwave field in the sample, $H_1^2 = 2.1$ G² with 0 dB attenuation, was calculated in accord with Ref. 14 taking into account the loaded Q of the cavity $Q_L = 5700$ and the microwave power dissipated in the cavity. The fields H_0 , H_1 , and H_2 acting on the sample were mutually orthogonal.

The microwave cavity had side apertures for passing through the crystal a probing-light beam parallel to H_0 . The source of light in the absorption band of the Tm^{2+} ion was an iodine incandescent lamp with filters isolating the spectral region $\lambda_{\text{max}} = 570$ nm, $\Delta\lambda = 25$ nm. The circular polarization of the light transmitted through the sample was modulated ($\sigma_+ \rightleftharpoons \sigma_-$) with a frequency ~ 50 kHz by a piezoelectric quartz modulator.¹⁵ A photodiode was used as the photodetector. Between the sample and the photodetector was placed a circular-polarization compensator consisting of a $\lambda/4$ plate and a linear polarizer.

In this work we investigated the high-field region of the EPR line: $H_0^{\text{max}} = 1950$ G for $\nu_1^{\text{micro}} = 8.910$ GHz.

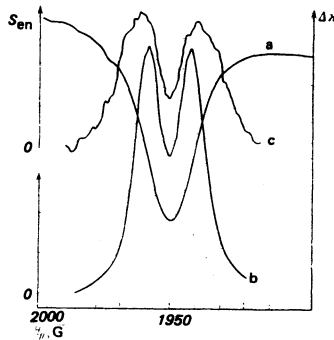


FIG. 1. (a) Optical detection EPR spectrum, $\Delta\kappa$, of the $\text{CaF}_2:\text{Tm}^{2+}$ crystal, sample No. 1, for a microwave field $H_1^2 = 2.1 \cdot 10^{-2}$ G² in the sample. (b) The intensity of the $\nu_2 = 12.13$ MHz line of the optical detection ENDOR spectrum $S_{en}(H_0)$ as a function of the external magnetic field, for the same sample. (c) $S_{en}(H_0)$ for sample No. 2, $\nu_2 = 12.13$ MHz, $H_1^1 = 2.1 \cdot 10^{-4}$ G².

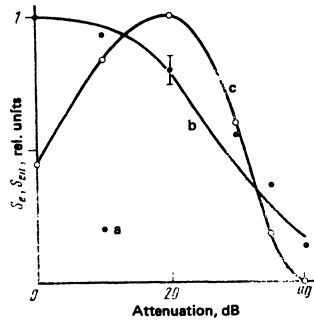


FIG. 2. (a), (b) Intensity of the optical detection EPR spectrum S_e . (c) Extremal (see Sec. 2) intensity of the $\nu_2 = 12.13$ MHz line of the optical detection ENDOR spectrum S_{en} in sample No. 1 as a function of the attenuation by the input attenuator of microwave power dissipated in the cavity, (a) experimental dependence and (b) calculated dependence from Eq. (4) for a value of the parameter $\tau_2 = 1.0 \cdot 10^{-7}$ s, (see text).

The optical detection EPR of the Tm^{2+} in CaF_2 (Fig. 1a) was recorded during measurement of the MCD¹⁾ ($\Delta\kappa$) in the region of the absorption band of the Tm^{2+} ion when the microwave power was turned on and the d.c. magnetic field H_0 was swept.

We studied the intensity and the width at half maximum of the optical detection EPR line as a function of the microwave field in the cavity. The experimental points (a) on Figs. 2 and 3 are the result of averaging several runs. The longitudinal relaxation time τ_1 of the electron spins in the crystals under study²⁾ was determined by the usual technique of recording the change with time of the MCD signal at the maximum of the optical detection EPR line after the microwave field was turned on¹ (see Table I).

In the study of the optical detection ENDOR, the field H_0 was set on the slope of the EPR line and the MCD signal was cancelled out by rotating the polarizer in

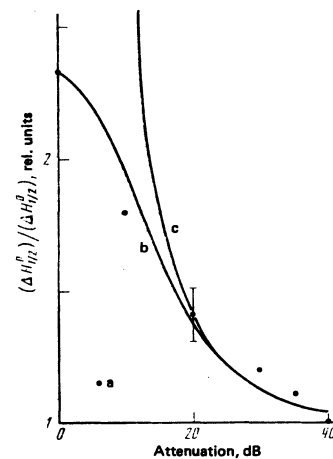


FIG. 3. Relative width $H_1^2/2 / H_1^1/2^0$ of the optical detection EPR line in sample No. 1 as a function of the attenuation of microwave power dissipated in the cavity. (a) experimental and (b), (c) calculated dependences (see text) for values of the parameters: (b) $\tau_2 = 4.0 \cdot 10^{-7}$ s, $\alpha\omega_{SS}^2 = 3.94 \cdot 10^{17}$ s⁻²; (c) $\tau_2 = 4.0 \cdot 10^{-7}$ s, $\beta_{SS} = 0$.

the compensating apparatus. With increasing cancellation of the MCD, the sensitivity of the amplifier recording the MCD increased by 1–2 orders of magnitude. Then an application of an amplitude-modulated ($\nu_{\text{modulation}} \sim 17$ Hz) rf field H_2 at the frequency of the most intense ENDOR line led to an appreciable change in the cancelled MCD, so that the optical detection ENDOR signal could be observed on the oscilloscope.³⁾

In Fig. 4 we give a typical optical detection ENDOR spectrum for the Tm^{2+} ion in CaF_2 . The spectrum has a shape typical of ligand ENDOR spectra of rare-earth ions in CaF_2 obtained by traditional methods.⁹ The weak intensity of a line which may be assigned to the "distant" nuclei (ν_p) is worthy of note. As was to be expected, optical detection ENDOR spectra are highly sensitive ($\sim 0.1^\circ$) to the orientation of the crystallographic axis of the samples relative to the direction of H_0 . The lowest observable width of the optical detection ENDOR line was ~ 30 kHz, and some lines were markedly broadened with increase of the rf field. (For example, the line $\nu_2 = 5.70$ MHz in sample No. 1 was broadened from 45 to 75 kHz as $H_2 \rightarrow 2$ G. At the same time, the shape of the $\nu_2 = 12.13$ MHz line was insensitive to a change in the rf field strength.)

On Figs. 1b and 1c we give the intensity of the optical detection ENDOR line $\nu_2 = 12.13$ MHz as a function of the d.c. magnetic field H_0 in the region of the optical detection EPR line of the Tm^{2+} ion. In measuring this dependence, the rf frequency was tuned to the maximum signal as H_0 was varied ($\sim 12.2 < \nu_2 < 12.0$ MHz).

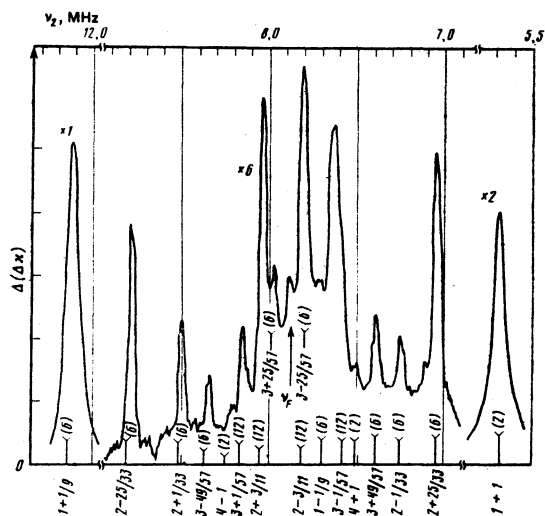


FIG. 4. Change $\Delta(\Delta\kappa)$, in the magnetic circular dichroism on the slope of the optical detection EPR line ($H_0 = 1967$ G) of the $\text{CaF}_2:\text{Tm}^{2+}$ crystal (sample No. 3) as a function of the frequency of the additional rf field of strength $H_2 = 2$ G (optical detection ENDOR spectrum). Microwave field parameters in the sample are $H_1^2 = 2.1 \cdot 10^{-2}$ G², $\nu_1 = 8.910$ GHz; $H_0 \parallel \langle 111 \rangle$. Underneath is given the position of the ENDOR lines calculated according to Eq. (6) (see text) using the hyperfine coupling constants.¹¹ Indicated are: the coordination sphere of the anion, the sign of the spin $S_x = \pm \frac{1}{2}$, of the electron shell of Tm^{2+} ; the value of $\cos^2\theta$, where θ is the angle between H_0 and the direction of the Tm^{2+} ion— F^- ion bond, and also (in parentheses) the number of equivalent F^{19} nuclei corresponding to the given ENDOR line.

On Fig. 2c we give the extremal intensity of the line $\nu_2 = 12.13$ MHz of the optical detection ENDOR spectrum as a function of the saturating microwave field. In plotting this dependence, we looked for the maximum value of the optical detection ENDOR signal with the magnetic field H_0 varied on the slope of the optical detection EPR line.

On Fig. 5 we give the intensity of several optical detection ENDOR lines as a function of the rf field H_2 . The maximum value of the optical-detection ENDOR signal for $H_2 \sim 2$ G was observed on the line $\nu_2 = 12.13$ MHz and was ~ 5 – 10% of the limiting intensity of the optical detection EPR signal at the maximum.

In studying on the oscilloscope screen the change with time of the optical detection ENDOR signal in the line $\nu_2 = 12.13$ MHz with an amplitude-modulated rf field, we observed that the optical detection ENDOR signal in this case is a saw-toothed curve with respect to time having approximately equal signal rise and decay times. The measured decay time for the ENDOR signal when the rf field is turned on (i.e., the time in which the optical detection ENDOR signal drops by a factor of e) in sample No. 2 is $\tau_3 \approx 5 \cdot 10^{-2}$, which leads to the relation $\tau_3 \sim \tau_1/2$ (see Table I).

3. DISCUSSION OF RESULTS

In studying the EPR spectra by optical detection methods, we detect the change in the total magnetic moment of the electron spin system relative to the equilibrium values at a lattice temperature T_L :

$$S_e(\Delta, H_1^2) = \frac{M_z^0 - M_z}{M_z^0} = \int \left[1 - \frac{\beta(\omega, \Omega)}{\beta_L} \right] \cdot G(\omega - \omega_0) d\omega. \quad (1)$$

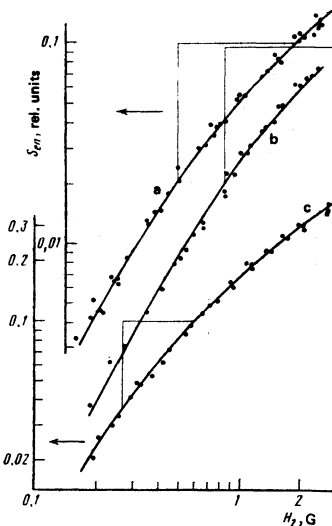


FIG. 5. Experimental (points) and calculated (solid lines) line intensities of the optical detection ENDOR spectrum $S_{em}(H_2)$; as a function of the amplitude of the rf field $H_2^2 = 2.1 \cdot 10^{-2}$ G². (a) sample No. 2, optical detection ENDOR spectral line $\nu_2 = 12.13$ MHz, for the calculated curve the value of the parameter is $\bar{\tau}_2 T_2^{-1} = 50$; (b) No. 1, $\nu_2 = 12.13$ MHz, $\bar{\tau}_2 T_2^{-1} = 50$; (c) No. 1, $\nu_2 = 5.70$ MHz, $\bar{\tau}_2 T_2^{-1} = 30$ (T_2^{-1} is the halfwidth of the optical detection ENDOR line). For the calculated curves, we indicate the value of the field $H_2^{(0)}$ at which $(1/4) \gamma_2^2 H_2^2 \bar{\tau}_2 = 1$, and also the position of the signal level corresponding to 0.1 of the limiting S_{em}^{max} .

Here, $\beta_L = (T_L)^{-1}$, $\beta(\omega, \Omega)$ is the reciprocal temperature of a spin packet of frequency ω in an inhomogeneous EPR line $G(\omega - \omega_0)$, for microwave pumping of intensity H_1^2 and frequency Ω ; $\Delta = \Omega - \omega$.

Assuming a Gaussian shape for the inhomogeneous EPR line, which is correct in our case, the distribution of resonant transition frequencies for the Tm^{2+} ions is described by the expression

$$G(\omega - \omega_0) = \left(\frac{\ln 2}{\pi}\right)^{1/2} T_2 \exp\{-\ln 2 \cdot T_2^2 (\omega - \omega_0)^2\}, \quad (2)$$

where ω_0 is the extremum and T_2^{-1} is the halfwidth of the inhomogeneous distribution. For the investigated high-field EPR line, the transition frequency and the static magnetic field are related by $\omega_0 \approx \gamma_1 H_0^{\max} - \pi A_{IS}$, where $\gamma_1 = g\beta/\hbar$ is the gyromagnetic ratio.

Neglecting spectral diffusion⁷

$$\beta(\omega, \Omega) = \left[\beta_L + \frac{\omega - \Omega}{\omega} \frac{\pi s}{\tau_2} g(\Omega - \omega) \beta_{SS}(\Delta) \right] \left[1 + \frac{\pi s}{\tau_2} g(\Omega - \omega) \right]^{-1}, \quad (3)$$

where $g(x)$ is the normalized spin-packet lineshape function which we usually assume to be Lorentzian

$$g(x) = \frac{\tau_2}{\pi} \frac{1}{1 + \tau_2^2 x^2};$$

the saturation parameter $s = (1/4)\gamma_1^2 H_1^2 \tau_1 \tau_2$; $\beta_{SS}(\Delta)$ is the reciprocal temperature of the dipole-dipole reservoir.

In order to determine τ_2 , we usually study the intensity of the optical detection EPR signal at the maximum ($\Delta = 0$) as a function of the saturating microwave field. In this case $\beta_{SS} = 0$, which leads to the known Portis theory¹⁶ applied to the optical detection EPR spectrum¹⁷:

$$S_e(H_1^2) = \left(\frac{\ln 2}{\pi}\right)^{1/2} T_2 \int_{-\infty}^{\infty} \frac{1/4 \gamma_1^2 H_1^2 \tau_1 \tau_2 \exp(-\ln 2 \cdot T_2^2 \omega^2) d\omega}{1 + 1/4 \gamma_1^2 H_1^2 \tau_1 \tau_2 + \tau_2^2 \omega^2}. \quad (4)$$

Since T_2 , τ_1 , γ_1 , and H_1^2 may be determined independently, comparison of the experimental dependence of $S_e(H_1^2)$ with that calculated in Eq. (4) on varying τ_2 allows us to estimate the transverse relaxation time τ_2 if spectral diffusion is neglected. As the examination in Ref. 7 shows, spectral diffusion may be neglected if the hole burned in the inhomogeneous line is greater than the spectral diffusion length: $\delta_s = (1 + s^2)^{1/2} / \tau_2 \gg l_{CR}$. Therefore, in order to determine τ_2 in the case of restricted spectral diffusion ($l_{CR} < T_2^{-1}$) it is desirable to use the region of the maximum optical detection EPR signal: $S_e \rightarrow 1$ when $\delta_s \sim T_2^{-1}$. In studying the S_e dependence in a broader region, $S_e = 0-1$, we must bear in mind that any manifestation spectral diffusion (caused by cross relaxation of resonant electron spins or non-resonant electron spins with participation of nuclear spins¹⁸), and also excitation of "forbidden" electron-nuclear transitions upon saturation of the EPR line, leads to an increase in S_e and consequently to a decrease in the experimental value of τ_2 . The value of $\tau_2 \approx 1 \cdot 10^{-7}$ s obtained from an analysis of the $S_e(H_1^2)$ dependence for sample No. 1 (see Figs. 2a, b) must thus be considered as a lower-bound estimate of the true value. This estimate is evidence that restricted (not rapid) spectral diffusion occurs in sample No. 1, since⁴ it turns out that $\tau_2^{-1} \ll T_2^{-1}$.

The analysis of the optical detection EPR line broadening as a function of the magnitude of the microwave field is of special interest, since in this case $\Delta \neq 0$ and we must take into account cooling of the dipole-dipole reservoir^{7,8}: $|\beta_{SS}/\beta_L| \gg 1$. Bearing in mind the analysis of results on the optical detection EPR line broadening in samples with restricted spectral diffusion in strong microwave fields, when $\delta_s \geq T_2^{-1} \gg l_{CR}$, we calculate β_{SS}/β_L as a function of saturation s and detuning Δ by using an expression^{7,8} in which the spectral diffusion is not taken into account:

$$\frac{\beta_{SS}}{\beta_L} \approx \frac{\int \omega' (\omega' - \Omega) G(\omega' - \omega_0) F(\omega' - \Omega, s) d\omega'}{a \omega_{SS}^2 + \int (\omega' - \Omega)^2 G(\omega' - \omega_0) F(\omega' - \Omega, s) d\omega'} \quad (5)$$

$$F(\omega' - \Omega, s) = \frac{(\pi s / \tau_2) g(\omega' - \Omega)}{1 + (\pi s / \tau_2) g(\omega' - \Omega)},$$

where ω_{SS} is the average frequency of the dipole-dipole reservoir and $a = \tau_1 / \tau_1'$, where τ_1' is the spin-lattice relaxation time of the dipole-dipole reservoir.

The experimental dependence of the optical detection EPR linewidth on the magnitude of the microwave field for the studied samples is substantially flatter than could be expected on the basis of the Portis theory without taking into account the dipole-dipole reservoir ($\beta_{SS} = 0$). This may be explained on the basis of Eqs. (1)-(3) and (5); from a comparison of the experimental and calculated dependences we may determine the parameters⁵ $a \omega_{SS}^2$ and τ_2 (see Fig. 3 and Table I). Analysis of Eq. (5) using the values obtained for the parameters $a \omega_{SS}^2$ and τ_2 allows us to state that the cooling of the dipole-dipole reservoir, for degrees of detuning Δ corresponding to points at which the observed optical detection EPR linewidth is measured (for $\delta_s \geq T_2^{-1}$), is close to the extremal value at the given microwave field level. The extremal value of β_{SS}/β_L increases monotonically with an increase in the microwave field, and at 0 dB attenuation it approaches the limiting value (as $s \rightarrow \infty$)⁶ given in Table I. For sample No. 1, $\beta_{SS}/\beta_L = 41.7$ at 0 dB attenuation. We must note that in our work we did not attain that critical level of saturation at which the optical detection EPR lineshape stops changing with an increase in the microwave field (see, for example, Ref. 5).

The parameter $\tau_2 \sim 4 \cdot 10^{-7}$ s for sample No. 1 (see Fig. 3b) was estimated from the broadening of the optical detection EPR line for $\delta_s \geq T_2^{-1}$; therefore, as was to be expected, it is greater than the estimate of τ_2 from an analysis of the $S_e(H_1^2)$ dependence obtained for $\delta_s < T_2^{-1}$ (see above) and it must be considered as closer to the true value. The discrepancy of the estimates confirms the conclusion that the spectral diffusion in sample No. 1 is restricted. The value $\tau_2 \sim 4 \cdot 10^{-7}$ s for sample No. 1 agrees satisfactorily with the estimates of the broadening of the electron spin packets on the basis of the theory of moments¹⁹ applied to the nonresonant dipole-dipole interaction of paramagnetic ions ($\tau_2 \gg T_2$): $\tau_2 \approx (2n\gamma_1^2 \hbar)^{-1} \approx 5 \cdot 10^{-7}$ s.

Finally, the experimental estimates of the relaxation parameters for the studied samples are given in Table I.

The optical detection ENDOR lines (Fig. 4) were identified on the basis of the expression for the frequencies

of transitions with reorientation of the nuclear spin $|I_x| = 1/2$ of the ligand ion in an external magnetic field H_0 (Ref. 9):

$$v_{\pm} = \left[\left\{ -\frac{1}{2\pi} \gamma(F^{19}) H_0 \pm \frac{1}{2} [A_S + (3 \cos^2 \theta - 1) A_P] \right\}^2 + \frac{9}{4} \sin^2 \theta \cos^2 \theta A_P^2 \right]^{1/2}, \quad (6)$$

where $\gamma(F^{19}) = 2.517 \cdot 10^4 \text{ rad} \cdot \text{s}^{-1}$ is the gyromagnetic ratio for the F^{19} nucleus, the plus and minus signs correspond to respectively the $+1/2$ and $-1/2$ orientation of the electron spin in the field H_0 , and θ is the angle between H_0 and the paramagnetic ion–ligand direction. The values of the constants A_S and A_P (see Sec. 2) were taken from Ref. 11.

We did not carry out here a detailed analysis of the ENDOR mechanism. However, we note that if this mechanism is taken to be the spin-packet shift mechanism⁹ (in which the transfer of saturation over the inhomogeneous EPR line on excitation of ENDOR transitions is taken into account), then we can explain naturally such results as: 1) the increase in the saturation of the Tm^{2+} electron spin system (the decrease in M_x) on excitation of the ENDOR transitions, 2) the double-peaked dependence of the intensity of the optical detection ENDOR spectral line on the external magnetic field H_0 in the region of the inhomogeneous EPR line (Figs. 1c, b), and 3) the characteristic time $\tau_3 \sim \tau_1/2$ (see Sec. 2) in which the excess saturation of the electron spin packets dissipates when the rf field exciting the ENDOR transitions is turned on.

In our study of the optical detection ENDOR, no coupling between the dipole–dipole reservoir of the Tm^{2+} ions and the nuclear spins of the ligands appears. The following experimental facts are evidence for this: 1) the drop in intensity of the optical detection ENDOR spectrum with increase of H_1^2 (Fig. 2c) under conditions of cooling the dipole–dipole reservoir (see above), and 2) the non-zero intensity of the optical detection ENDOR spectrum upon microwave pumping at the center of the EPR line. We note that the weak intensity of the optical detection ENDOR at remote nuclei (see Sec. 2) is not evidence for weak coupling between the dipole–dipole reservoir and the nuclear Zeeman subsystem of remote nuclei, and is completely explained on methodological grounds, namely, the smallness of the period of the modulation the field H_2 compared with the polarization time of the remote nuclei upon microwave pumping.⁶

The intensity of the optical detection ENDOR spectrum, just as traditional ENDOR, obviously depends directly on the degree of saturation of the ENDOR transitions with reorientation of the nuclear spin of the corresponding ligand ions^{13, 21}; thus it is described for the inhomogeneous ENDOR line by a functional dependence analogous to Eq. (4).⁷ In our work, to determine the transverse relaxation time $\tilde{\tau}_2$ of the nuclear spin packet in the inhomogeneous ENDOR line, we studied the $S_{\text{en}}(H_2)$ dependence of the optical detection ENDOR line intensity at the maximum as a function of the rf field H_2 (see Fig. 5 and Table I). The value obtained from an analysis of the $S_{\text{en}}(H_2)$ dependence for the field $H_2^{(0)}$ at which the saturation parameter for the ENDOR line is $(1/4)\gamma_2^2 H_2^2 \tilde{\tau}_1 \tilde{\tau}_2 = 1$ (see Fig. 5) allows us to explain the

different broadening of the optical detection ENDOR spectral lines as the rf field increases (see Sec. 2), since the broadening $\Delta\nu(H_2) \propto (H_2/H_2^{(0)})\pi/\tilde{\tau}_2$.

It is interesting to note that the ratio of the experimental estimates of the transverse relaxation times of the electron spin packets in the EPR line and of the nuclear transverse relaxation times in the ENDOR line is $\tau_2/\tilde{\tau}_2 \sim \gamma(F^{19})/\gamma_1$.

The result is obviously evidence that the basic cause of the broadening of the electron and nuclear spin packets are the fluctuations in the local magnetic field due to the paramagnetic impurities distributed in the lattice.⁸⁾

4. CONCLUSION

Thus we have used optical detection methods to study the EPR and ENDOR spectra of the Tm^{2+} ion in CaF_2 upon exposure of the electron spin system of the Tm^{2+} ions to powerful microwave fields which are capable of inducing spin-temperature and dynamic nuclear polarization effects. We have studied the role of the dipole–dipole reservoir under conditions of saturation of the inhomogeneous EPR line with restricted spectral diffusion, and we have estimated the degree of cooling of the dipole–dipole reservoir from the broadening of the optical detection EPR line.

The essential features of the optical detection ENDOR spectra that we obtained are apparently explained by traditional mechanisms, and are not directly connected with cooling of the dipole–dipole reservoir by nonresonant microwave pumping. Comparison of the optical detection ENDOR spectra with the ENDOR spectra of the Tm^{2+} ions in CaF_2 obtained by traditional methods¹¹ shows that the sensitivity of the optical detection ENDOR method with detection based on MCD in the absorption bands under favorable conditions [the existence of absorption bands in the paramagnetic impurity with strong magnetic circular dichroism (MCD) in an accessible region of the spectrum] is apparently not inferior to the sensitivity of traditional methods. We should mention here that by now optical detection methods have been developed²³ that are 2–3 orders of magnitude more sensitive than the method used in our work.

The author thanks V. A. Atsarkin for useful discussions and valuable advice.

¹⁾ In the MCD measurement, one registers an alternating photodiode signal that corresponds to the difference in the transmission of right- and left-circularly polarized light by the sample.

²⁾ As is well known,¹⁰ the time τ_1 is shortened by 2–3 orders of magnitude in crystals containing a significant concentration of the diamagnetic heterovalent impurity Tm^{3+} .

³⁾ The intensity of the light signal in the studied samples was $\Delta\kappa \sim 6\%$ of the intensity of the light passing through the sample in the MCD measurement, $\Delta\kappa \sim 3\%$ in the measurement of the optical detection EPR, and $\Delta(\Delta\kappa) \sim 0.3\%$ for the optical detection ENDOR.

- ⁴In the fast spectral diffusion case ($l_{CR} > T_2^{-1}$), the analysis of the S_e dependence should lead to the incorrect result $\tau_2 \sim T_2$ (Ref. 19).
- ⁵The assumptions concerning the form of the function $g(x)$ exert an appreciable effect on the behavior of the calculated dependence. For example, a good fit to the experimental dependence Fig. 3a can be obtained without taking into account the dipole—dipole reservoir by formally assuming²⁰ that $g(x) = \tau_2/\pi \exp(-\ln 2 \cdot R^2 x^2) / (1 + \tau_2^2 x^2)$ for $R \approx T_2$, $T_2 = 1.0 \cdot 10^{-7}$ s.
- ⁶For $s \rightarrow \infty$, $F(\Omega - \omega, s) \rightarrow 1$, and $B = a\omega_{ss}^2 + (21n2 \cdot T_2^2)^{-1}$, we have $\beta_{SS}/\beta_L \approx -\omega_0 \Delta / (B + \Delta^2)$ and $S_e = 1 - \Delta^2 / (B + \Delta^2)$, so that $|\beta_{SS}/\beta_L|^{max} = \omega_0 / 2B^{1/2}$ is attained for $\Delta^2 = B$, when $S_e = 1/2$. We note that β_{SS}/β_L and S_e do not depend explicitly on τ_2 as $s \rightarrow \infty$.
- ⁷For the reasons for the inhomogeneous broadening of the ENDOR lines, see Ref. 22.
- ⁸The broadening of the nuclear spin packet in the ENDOR line (which is connected with the finite lifetime of the central paramagnetic ion in the given spin state) is small, $\sim \tau_1^{-1} + \tau_0^{-1} < \tau_2^{-1}$, where τ_0^{-1} is the probability of cross relaxation of the paramagnetic ion. Calculations of τ_0^{-1} according to Ref. 18 for sample No. 1 lead to the value $\tau_0^{-1} \sim 1 \cdot 10^3$ s⁻¹.
- ¹S. Geschwind, in: *Electron Paramagnetic Resonance*, ed. by S. Geschwind, Plenum, New York, 1972, p. 353.
- ²L. F. Mollenauer and S. Pan, *Phys. Rev.* **B6**, 772 (1972).
- ³S. A. Kazanskiĭ, *Pis'ma Zh. Éksp. Teor. Fiz.* **29**, 525 (1979) [*JETP Lett.* **29**, 479 (1979)]; *Opt. Spektrosk.* **48**, 917, 1219 (1980) [*Opt. Spectrosc. (USSR)* **48**, 505, 668 (1980)].
- ⁴A. V. Komarov and S. M. Ryabchenko, *Zh. Éksp. Teor. Fiz.* **69**, 955 (1975) [*Sov. Phys. JETP* **42**, 485 (1975)].
- ⁵S. Z. Kazanskiĭ, *Pis'ma Zh. Éksp. Teor. Fiz.* **30**, 296 (1979) [*JETP Lett.* **30**, 274 (1979)].
- ⁶V. A. Atsarkin, *Usp. Fiz. Nauk* **126**, 3 (1978) [*Sov. Phys. Usp.* **21**, 725 (1978)]; V. A. Atsarkin and M. I. Rodak, *Usp. Fiz. Nauk* **107**, 3 (1972) [*Sov. Phys. Usp.* **15**, 251 (1972)].
- ⁷L. L. Buishvili, M. D. Zviadadze, and G. R. Khutsishvili, *Zh. Éksp. Teor. Fiz.* **56**, 290 (1969) [*Sov. Phys. JETP* **29**, 159 (1969)]; *Zh. Éksp. Teor. Fiz.* **54**, 876 (1968) [*Sov. Phys. JETP* **27**, 469 (1968)].
- ⁸V. A. Atsarkin and V. V. Demidov, *Zh. Éksp. Teor. Fiz.* **76**, 2185 (1979) [*Sov. Phys. JETP* **49**, 1104 (1979)].
- ⁹A. Abragam and B. Bleaney, *Electron Paramagnetic Resonance of Transition Ions* (International Series of Monographs on Physics), Oxford Univ. Press, New York, 1970 (Russ. transl., Mir, Moscow, 1972, Ch. 4, 5).
- ¹⁰E. S. Sabisky and C. H. Anderson, *Phys. Rev.* **B1**, 2028 (1970).
- ¹¹R. G. Bessent and W. Hayes, *Proc. Roy. Soc.* **A285**, 430 (1965).
- ¹²V. A. Arkhangel'skaya, M. N. Kiseleva, and V. M. Shraifber, *Opt. Spektrosk.* **23**, 509 (1967) [*Opt. Spectrosc. (USSR)* **23**, 275 (1967)].
- ¹³H. Siedel, *Z. Phys.* **165**, 218; 239 (1961).
- ¹⁴C. P. Poole, Jr., *Electron Spin Resonance: A Comprehensive Treatise on Experimental Techniques*, Interscience, New York, 1966 (Russ. Transl., Mir, Moscow, 1970, Ch. 2, Sec. 8, §5; Ch. 4, Sec. 8).
- ¹⁵S. N. Jasperson and S. E. Schnatterly, *Rev. Sci. Instrum.* **40**, 761 (1969).
- ¹⁶A. M. Portis, *Phys. Rev.* **91**, 1071 (1953); T. G. Castner, Jr., *Phys. Rev.* **115**, 1506 (1959).
- ¹⁷K. Murayama, K. Morigaki, and H. Kanzaki, *J. Phys. Soc. Japan* **38**, 1623 (1975).
- ¹⁸A. D. Milov, K. M. Salikhov, and Yu. D. Tsvetkov, *Fiz. Tverd. Tela (Leningrad)* **14**, 2259 (1972) [*Sov. Phys. Solid State* **14**, 1956 (1972)]; K. M. Salikhov, A. G. Semenov, and Yu. D. Tsvetkov, *Elektronnoe spinovoe ékho i ego primeneniye (Electron Spin Echo and Its Applications)*, Nauka, Novosibirsk, 1976, Ch. 3, Sec. 2.2.
- ¹⁹S. A. Al'tshuler and B. M. Kozyrev, *Elektronnyĭ paramagnitnyĭ rezonans (Electron Paramagnetic Resonance)*, Nauka, Moscow, 1972, Ch. 4 [Academic, 1964].
- ²⁰J. J. Markham, *F-Centers in Alkali Halides (Solid State Physics, Supplement 8)*, Academic Press, New York, 1966, Ch. 8, Sec. 21.
- ²¹V. L. Gokhman, V. Ya Zevin, and B. D. Shanina, *Fiz. Tverd. Tela (Leningrad)* **10**, 337 (1968) [*Sov. Phys. Solid State* **10**, 269 (1968)]; K. K. Pukhov, *Fiz. Tverd. Tela (Leningrad)* **21**, 1536 (1979) [*Sov. Phys. Solid State* **21**, 885 (1979)].
- ²²J. M. Baker and J. P. Hurrell, *Proc. Phys. Soc.* **82**, 742 (1963).
- ²³E. B. Aleksandrov and V. S. Zapasskiĭ, *Opt. Spektrosk.* **41**, 855 (1976) [*Opt. Spectrosc. (USSR)* **41**, 502 (1976)].

Translated by Cathy Flick